



Research Article

First and second law assessment of a solar tower power plant for electrical power production and error analysis

Mohd PARVEZ^{*1}, Syed Mohammed MAHMOOD², Osama KHAN²

¹Department of Mechanical Engineering, Al-Falah University, Haryana, India

²Department of Mechanical Engineering, Jamia Millia Islamia, New Delhi, India

ARTICLE INFO

Article history

Received: March 20, 2023

Revised: May 19, 2023

Accepted: May 24, 2023

Key words:

Heliostat field, steam cycle, waste heat recovery, exergy destruction, organic Rankine cycle

ABSTRACT

The primary objective of this study is to investigate the solar-powered combined-cycles system for converting the available solar energy to its truest potential and for generating electrical power. This combined-cycles system consists of a solar power tower, steam turbine cycle, and organic Rankine cycle. The study focuses on recovering the waste heat that is obtained from the exit of a steam turbine and using it to operate the Rankine cycle with refrigerants R-113, R-11, and R-1233zd. The analysis also predicts the effects of solar irradiance for a mass flow rate of molten salt and steam, turbine inlet pressure, and turbine inlet temperature on first and second law efficiencies in the combined-cycles system. The novel concept of uncertainty analysis is also introduced in this work in order to provide precise accurate results and remove all errors, which are found to be in the desired range of 3.81%. The results also show that as the direct normal irradiation (DNI) increases from 600 W/m² to 1000 W/m², first law efficiency is obtained in the range of 32.31% to 37.99% and second law efficiency from 24.14% to 25.51% after employing the organic Rankine cycle (ORC) system. Further, the results indicate the maximum exergy destruction that occurs in the central receiver to be around 42%, in the heliostat to be 31%, in the steam generator to be 10%, and in the heat exchanger to be 3.6%.

Cite this article as: Parvez M, Mahmood SM, Khan O. First and second law assessment of a solar tower power plant for electrical power production and error analysis. *Seatific* 2023;3:1:33–42.

1. INTRODUCTION

In the modern era, communities often opt for a sustainable approach to power generation that involves a responsible procedure for utilizing energy resources at bare minimum cost while simultaneously posing lower detrimental environmental effects. The front runners for conventional fuels are fossilized coal, petro-diesel products, and compressed natural gas, which have been utilized for decades in energy generation across the globe but are acknowledged as being finite, and side effects such as global warming and climate change are associated with their applications in the power industry (Parvez, 2017; Vujanović et al., 2019; Kumar, 2020; Assad & Rosen, 2021). To meet

these challenges, an urgent need exists for developing cost-effective energy alternatives. Based on the above energy perspective, concentrating on solar thermal setups seems to be an attractive perspective and feasible enough to fulfil and simultaneously achieve cleaner economical power generation with a lower global environmental impact (Hussaini et al., 2020; Ayaz et al., 2021; Akram et al., 2023).

Over the past few years, a large number of studies have been devoted to developing various technologies to provide a viable and feasible solution for harnessing the potential of thermal radiation. One of these technologies was seen in the development of a central receiver system that primarily deploys a substantial number of heliostat field solar collectors

*Corresponding author.

*E-mail address: mparvezalig@rediffmail.com



integrated with solar receivers and placed at the zenith of a solar tower (Collado & Guallar, 2019; Ahmad et al., 2022; D'Souza et al., 2023). This integrated system employs a working fluid primarily in molten salt or Duratherm oil, thereby deploying first-of-their kind grid-connected commercial solar power plants (Zolfagharnasab et al., 2020; Caraballo et al., 2021).

In the past, multiple studies have established steam turbines as the prime component for utilizing the maximum amount of energy compared to other equipment, predominantly due to the majority of heat being carried away in the form of flue gases. Generally, these gases have comparatively higher temperatures than atmospheric conditions; as a result, heat transfer leads to substantial energy losses and further leads to lower efficiency rates (Omar et al., 2019; Corumlu & Oztur, 2021; Varis & Ozkilic, 2023).

Successful models have been developed to curb energy losses while simultaneously utilizing this waste energy. Among these models, the conventional organic Rankine cycle (ORC) system has been found to be quite effective in successfully recovering waste heat sources. ORCs provide an improved method for successfully transforming the waste heat energy accessible at the exit of the steam turbine into electrical power. This system works with an organic, high molecular mass working fluid that possesses the characteristics of having a liquid-vapor phase change (i.e., boiling point) that occurs at temperatures below the water-steam phase transformation temperature (Haq, 2021; Zheng et al., 2022; Li et al., 2023). ORCs do not consume additional energy and reduce environmental pollution factors such as CO₂ and SO₂. In recent years, many researchers have considered thermodynamic assessments in order to utilize solar energy as a major source for power production integrated with ORC to enhance the performance of the entire system (Singh & Mishra, 2019; Lourenco, 2023).

Georges et al. (2013) designed a small-scale ORC integrated with an engine solar power plant that used techniques to optimize and regulate the policies that should be employed for larger systems. Their study focused on simulated replicas of the ORC engine while simultaneously considering its basic limitation that restricts a wider range of operating temperatures and technical maturity of the components. These prospective simulations allowed the efficiency of the ORC engine to be able to shoot up to 12% when the evaporating and condensing temperatures lie respectively between 140°C and 358°C. Li (2014) investigated a simple ORC technology operated by a low-grade heat source for converting heat to power. The basic principle behind ORC is quite analogous to a simple steam Rankine cycle. The organic working fluid is pumped into the heat exchanger where it can be vaporized. Furthermore, Li equated the results with the conventional steam Rankine cycle, showing ORC to have numerous benefits. Kerme and Orfi (2015) explained a different system for enabling thermodynamic modeling for conventional ORCs primarily operated by parabolic trough solar collectors for testing eight different kinds of working fluids. They also independently investigated the most influential parameters such as turbine inlet temperature on turbine size, expansion ratio, outlet volume flow rate, irreversibility ratio, and total exergy destruction. Consequently, the results

obtained from their study showed that the maximum exergy destruction occurred in the solar collector with about 74.9% of the total exergy destroyed, and the next 18.2% of the total destroyed exergy occurring in the condenser. Loni et al. (2017) carried out an exergy analysis of an ORC that receives radiated thermal energy from the tubular cavity receiver of a solar dish collector. The analysis performed in their study was checked with several parameters such as receiver exergy rate, receiver exergy factor, thermal exergy efficiency, and electrical exergy efficiency.

Studies on exergy analysis for minimizing losses in power plants have provided valuable insights into the energy losses that occur within a system. By employing exergy analysis techniques, researchers can gain a comprehensive understanding of the thermodynamic inefficiencies present in power plant equipment. This knowledge allows one to identify the specific areas where improvements can be made in order to optimize energy conversion processes and reduce unnecessary energy dissipation. By focusing on exergy analysis, researchers can develop innovative strategies and technologies to limit losses, leading to increased operational efficiency, reduced environmental impacts, and improved economic viability for power plants. Such studies play a vital role in enhancing the overall efficiency and sustainability in the power generation sector.

Recently, a majority of researchers have investigated the heat recovery ORC cycle operated with regard to various working fluids and using solar energy as the prime source for running the system. Doe et al. (2022) focused on investigating the exergy losses in various components and exploring strategies to improve overall efficiency. They proposed modifications to the system design and operating parameters based on their exergy analysis findings to reduce losses and enhance the energy conversion process. Habibi et al. (2020) investigated a regenerative supercritical Brayton cycle with an organic Rankine cycle attached at the bottom and the cycle driven by a solar power tower applying molten salt as a working refrigerant. The results show the maximum exergy efficiency obtained to be 21.23%; a net power output of 177,321 kW should be achievable when helium is used as a refrigerant, and the highest exergy destruction is provided at 70,576 kW obtained from oxygen. Yağlı et al. (2021) presented an ORC system to improve the entire performance of a gas turbine used in wood production. A steam boiler cycle was integrated with a gas turbine alongside an ORC to produce steam to run the cycle. Their results indicate that the maximum ORC net power production, thermal efficiency, and exergy efficiency were found to respectively be 1,076.76 kW, 21.14%, and 47.00% after employing the ORC using R123 as a working fluid at 230°C and 35 bars of pressure. Chen et al. (2022) recently published a paper on a solar-based hybrid energy system for producing electrical energy, thermal energy, and hydrogen fuel. Their computed results revealed the system to be able to generate 147.8 kWh/day of electrical energy and 595 g/day of hydrogen fuel. The past available literature shows studies to have seldom been conducted on the ORC cycle integrated with the heliostat field's solar collector for power generation in terms of first and second law analyses.

Table 1. Properties of the solar-operated steam Rankine cycle-ORC configuration combined-cycles system (Ahmad et al., 2022; Akram et al., 2023)

System properties values		
Heliostat field	Beam radiation (DNI; mid value)	800 W/m ²
	Overall field efficiency	75%
	Total heliostat aperture area	10,000 m ²
Central receiver	Aperture area	12.5 m ²
	Inlet temperature of molten salt	290°C
	Outlet temperature of molten salt	565°C
	View factor	0.8
	Tube diameter	0.019 m
	Tube thickness	0.00165 m
	Emissivity	0.8
	Reflectivity	0.04
	Wind velocity	5.0 ms ⁻¹
	Passes	20
Steam generator	Internal temperature of water	240°C
	Outlet temperature of steam	550°C
	Ambient temperature	20°C
Organic Rankine cycle	Working fluid used in ORC	R-113, R-11, R-1233zd
	Mass flow rate of waste heat source	1 kg/s
	ORC turbine inlet pressure (bar)	15-35 (range)
	ORC turbine outlet pressure (bar)	0.5
	ORC turbine isentropic efficiency	80%
	ORC pump isentropic efficiency	75%
Thermo-physical properties of molten salt	Temperature range of molten salt	220°C-574°C
	Viscosity of molten salt	25 MPa-s
	Density of molten salt	863 Kg/m ³
	Thermal conductivity of molten salt	0.134 W. K ⁻¹ .m ⁻¹
	Specific heat of molten salt	10 kJ.K ⁻¹ .kg ⁻¹
	Freezing temperature of molten salt	238°C

ORC: Organic Rankine cycle; DNI: Direct normal irradiation

The current study’s primary objective is to evaluate the first and second law analyses of ORC driven with input energy from the waste heat available at the exit of the steam turbine that receives energy from a heliostat field’s solar collector. The study further includes the various numerical calculations that form the basis of the graphs plotted to understand and thus comment on the relationships among various properties. The article conducts a detailed study of first and second law analyses on ORC using the refrigerants R-113, R-11, and R-1233zd and applies a proper uncertainty analysis in order to eliminate any adherent errors so as to enhance the accuracy of this analysis. Table 1 shows the properties of the solar-operated steam Rankine cycle-ORC configuration combined-cycles system.

2. SYSTEM DESCRIPTION

The planned solar-operated system contains a steam Rankine cycle (RC) and an organic cycle Rankine (ORC) operating with the aid of solar energy to generate electricity. Figure 1 shows the outline of the entire system. With regard to the solar components, they are comprised of a set of heliostats that collect and concentrate sunlight onto the

receiver, which captures the focused sunlight and transfers the heat energy to the working fluid (molten salt). This heat transportation system is comprised of primary pipes, pumps, and valves and facilitates the heat transfer to the power conversion systems. The power transformation system is comprised of a steam generator, turbine generator, organic Rankine system and supplies different types of apparatuses that convert the thermal energy into electric power and further supplies it to the utility grid.

The molten salt enters at high temperature into a steam generator, where it transfers the thermal energy, thereby generating steam that is in turn expanded to generate electric power in a steam turbine. The waste heat of the steam obtained at the exit of the steam turbine moves into the heat exchanger, where it then transfers its remaining heat for recovery by running the ORC system, after which the saturated liquid is pumped to the steam generator of the RC cycle. Furthermore, the steam exits from the heat exchanger where the heated organic vapor enters the refrigerant turbine and produces power as it expands. Furthermore, this thermal energy is transferred into the atmosphere within the condenser, allowing lowered temperature refrigerant into the heat exchanger to complete the cycle.

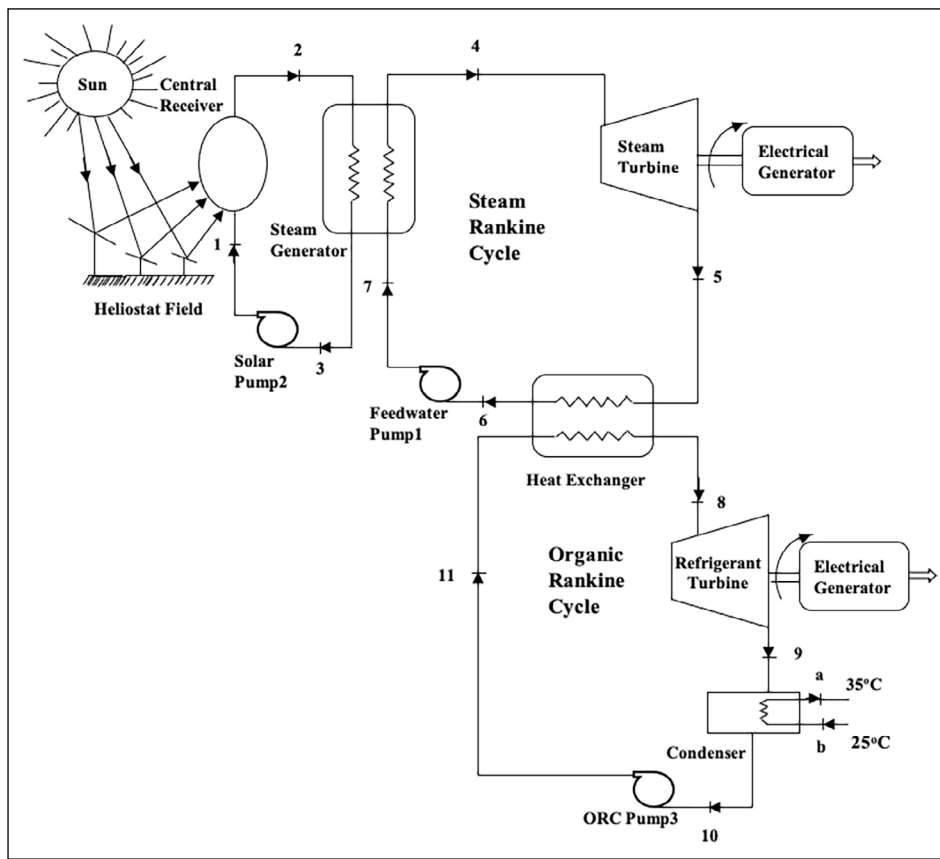


Figure 1. Solar tower power plant.

ORC: organic Rankine cycle.

3. UNCERTAINTY ANALYSIS

The primary reason for carrying out an error and uncertainty analysis in any research is that human errors are very common, and even machines may have some small errors in the calculation of a property that also needs to be taken into consideration and calibrated likewise. Table 2 displays all the equipment used for measuring various properties in the system along with its errors.

The total percentage of uncertainty (TPU) has been determined in this experiment by applying the equation (Holman, 2012) provided below:

$$TPU = [(U_1)^2 + (U_2)^2 + (U_3)^2 + (U_4)^2 + (U_5)^2 + (U_6)^2]^{0.5} \quad (1)$$

As a result, the total uncertainty associated with the system comes close to 3.81% for which the analysis of a complete setup is suitable, satisfactory, and in line with previous research (Holman, 2012; Seraj, 2022).

4. THERMODYNAMIC MODELING FOR A COMBINED-CYCLES SYSTEM FOR ELECTRICAL POWER PRODUCTION

This study mainly focuses on the primary model of a cascade system that is based on the integration of two varying models with one another. Analysis of the first and second laws has been carried out for mass, energy, and exergy balances, which will enable pinpointing the exact location

within the model where components may have maximum thermodynamic inefficiencies. The study has formulated some basic assumptions and explained them as follows:

- The complete model is an integration of different components aligned together to work as a single model and is further presumed to work at a steady-state condition with constant solar insulation.
- During the entire analysis, the ambient conditions in which the model operated assume standard and constant values of temperature T_0 and pressure p_0 at 20.3°C and 1.01325 bar.
- Subsequent pressure drops and thermal losses in the atmosphere have not been taken into consideration for the majority of the model's apparatuses.
- Sudden variations or alterations in the potential and kinetic-based energies have not been considered within the study's formulations.
- The chemical exergy associated with the materials has not been taken into consideration.

4.1. Heliostat (H)

The heliostat field is an integration of several stacked-up heliostats that represent and focus the majority of the sun's rays onto the centralized dedicated receiver. The rate at which a major portion of solar thermal input is being received may be written as:

Table 2. Measurement accuracies and experimental uncertainties associated with sensors and parameters

Sensor no	Sensors and parameters	Designated symbol	Accuracies and uncertainties measurement
1	T-type thermocouples	U_1	± 0.3 C
2	Flow meter	U_2	± 4 ml
3	Pressure transducer	U_3	± 1.9 m bar
4	Voltage measurement	U_4	± 0.08 V
5	Current measurement	U_5	± 0.1 A
6	Power temperature coefficient	U_6	$-0.3\%/C$

$$\dot{Q}_{solar} = A_{field} q \quad (2)$$

where q is the amount of solar radiation received per unit area and A_{field} is the calculated area of the heliostat field. This is linked to the field of opening (A_{app}) in terms of the concentration ratio and is written as follows:

$$C = \frac{A_{field}}{A_{app}} \quad (3)$$

The central receiver receives half of the thermal energy obtained from the heliostat, with the remainder being lost to the atmosphere and expressed as:

$$\dot{Q}_{solar} = \dot{Q}_{CR} + \dot{Q}_{lost, heliostat} \quad (4)$$

The heliostat's energy efficiency is written as:

$$\eta_{energy, heliostat} = \frac{\dot{Q}_{CR}}{\dot{Q}_{solar}} \quad (5)$$

The thermal energy from the central recipient that is consequently drained into the atmosphere by the molten salt with the remainder being lost is expressed as follows:

$$\dot{Q}_{CR} = \dot{Q}_{moltensalt} + \dot{Q}_{lost, CR} = \dot{m}_{moltensalt} (h_2 - h_1) + \dot{Q}_{lost, CR} \quad (6)$$

$$\eta_{energy, CR} = \frac{\dot{m}_{moltensalt}}{\dot{Q}_{CR}} \quad (7)$$

The exergy destruction in the central receiver is written as:

$$\Delta \dot{E}_{CR} = \dot{m}_{moltensalt} [(h_2 - h_1) - T_0 (s_2 - s_1)] \quad (8)$$

4.2. Steam generator (SG)

Using the energy balance approach to a steam generator results in:

$$\dot{m}_{moltensalt} (h_2 - h_3) = \dot{m}_{st} (h_4 - h_5) \quad (9)$$

The exergy destruction in the heat steam generator is expressed as:

$$\Delta \dot{E}_{SG} = T_0 [\dot{m}_{moltensalt} (s_2 - s_3) + \dot{m}_{st} (s_4 - s_7)] \quad (10)$$

4.3. Steam turbine (ST)

Applying the first law of thermodynamics to the steam turbine results in:

$$\dot{W}_T = \dot{m}_{st} (h_4 - h_5) \quad (11)$$

The exergy destruction in the steam turbine is expressed as:

$$\Delta \dot{E}_{st} = \dot{m}_{st} [(h_4 - h_5) - T_0 (s_4 - s_5)] - \dot{W}_T \quad (12)$$

4.4. Heat exchanger (HE)

The energy balance regarding the heat exchanger is expressed as:

$$\dot{m}_{st} (h_5 - h_6) = \dot{m}_{ref} (h_8 - h_{11}) \quad (13)$$

The exergy destruction in the heat exchanger is written as:

$$\Delta \dot{E}_{HE} = T_0 [\dot{m}_{st} (s_5 - s_6) + \dot{m}_{ref} (s_8 - s_{11})] \quad (14)$$

4.5. Feedwater pump1 (FWP1)

The energy balance regarding the feedwater pump1 is expressed as:

$$\dot{W}_{FWP1, wt} = \dot{m}_{wt} (h_7 - h_6) \quad (15)$$

The exergy destruction in the feedwater pump is written as:

$$\Delta \dot{E}_{FWP1} = T_0 [\dot{m}_{wt} (s_7 - s_6)] \quad (16)$$

4.6. Solar pump2 (SP₂)

The energy balance regarding the solar pump is expressed as:

$$\dot{W}_{SP2} = \dot{m}_{solarfluid} (h_3 - h_1) \quad (17)$$

The exergy destruction in the solar pump is written as:

$$\Delta \dot{E}_{SP2} = T_0 [\dot{m}_{solarfluid} (s_3 - s_1)] \quad (18)$$

4.7. Refrigerant turbine (RT)

The energy balance regarding the refrigerant turbine is expressed as:

$$\dot{W}_{T, RT} = \dot{m}_{vapour} (h_8 - h_9) \quad (19)$$

The exergy destruction in the refrigerant turbine is written as:

$$\Delta \dot{E}_{RT} = \dot{m}_{RT} [(h_8 - h_9) - T_0 (s_8 - s_9)] - \dot{W}_{T, RT} \quad (20)$$

4.8. Condenser (C)

The energy balance regarding the condenser is expressed as:

$$\dot{m}_{vapour} (h_9 - h_{10}) = \dot{m}_{water} (h_a - h_b) \quad (21)$$

The exergy destruction in the condenser is written as:

$$\Delta \dot{E}_C = T_0 [\dot{m}_{vapour} (s_9 - s_{10}) + \dot{m}_{water} (s_a - s_b)] \quad (22)$$

4.9. ORC pump3 (ORC P3)

The ORC pump's energy balance is expressed as follows:

$$\dot{W}_{ORC, P3} = \dot{m}_{ref} (h_{11} - h_{10}) \quad (23)$$

The depletion of exergy in the solar pump is calculated as follows:

$$\Delta \dot{E}_{ORC, P3} = T_0 [\dot{m}_{ref} (s_{10} - s_{11})] \quad (24)$$

4.10. First law efficiencies

First law efficiencies is the ratio of useful energy produced in the entire system to the input energy of the fuel supplied to the entire system, can be written as:

$$\eta_I = \frac{\dot{W}_{ST} + \dot{W}_{RT} - \dot{W}_{SP1} - \dot{W}_{SP2} - \dot{W}_{ORC, P3} - \dot{W}_{C, ORC}}{\dot{Q}_{C, R}} \quad (25)$$

4.11. Second law efficiencies

The product exergy output is known as the exergy input separated into the whole system and calculated as:

$$\eta_{II} = \frac{\dot{W}_{ST} + \dot{W}_{RT} - \dot{W}_{SP1} - \dot{W}_{SP2} - \dot{W}_{ORC, P3} - \dot{W}_{C, ORC}}{\dot{E}_{x, in}} \quad (26)$$

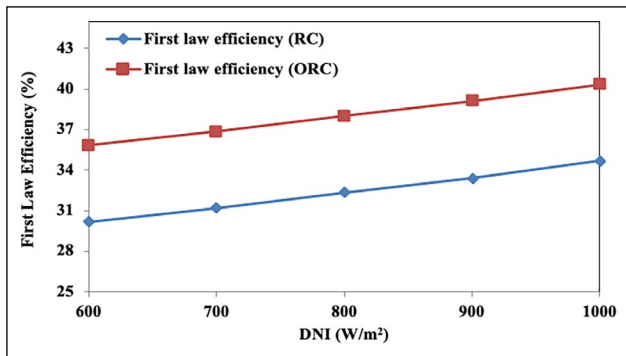


Figure 2. Variations in first law efficiencies with changes in DNI of an RC and ORC solar tower power plant.

DNI: Direct normal irradiation; RC: Rankine cycle; ORC: Organic Rankine cycle.

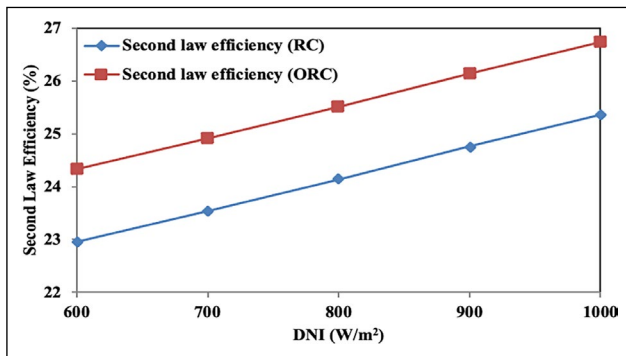


Figure 3. Variation of second law efficiency with the change in DNI of an RC and ORC solar tower power plant.

5. DEFINING RESULTS AND DISCUSSIONS

This section explains the basic framework and evaluates the estimations after employing thermodynamic modeling for the first and second law analyses. Furthermore, this section computes a combined assessment of the effects on the several important parameters that furnish a major effect on the results of solar-powered combined cycles. To complete this study, influential parameters have been analyzed such as the effect of solar irradiance on first and second law efficiencies, the mass flow rate of molten salt and steam, turbine inlet pressure, turbine efficiencies at the inlet, and exergy degradation regarding the first and second laws regarding all major modules within the combined-cycles system. The study has also examined the thermodynamic properties of refrigerants R-113, R-11, and R-1233zd as procured in the ORC cycle, and the results are well-matched under similar conditions (Parvez & Khalid, 2018; Shah et al., 2020).

The effects of first and second law efficiencies alongside changes in the direct normal irradiation (DNI) on a steam Rankine cycle and organic Rankine cycle of a combined-cycles system are summarized in Figures 2 and 3. The efficiency of an entire system is increased by increasing the DNI values from 600 W/m² to 1,000 W/m². This observation results from an extreme sensitivity while considering the dissimilarity of DNI captured from the

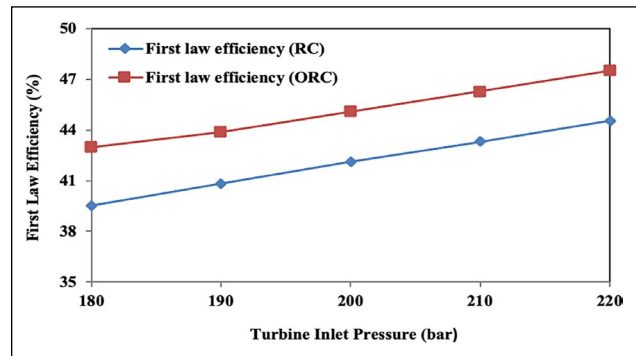


Figure 4. Variations in first law efficiencies with changes in the turbine inlet pressure of the solar tower power plant.

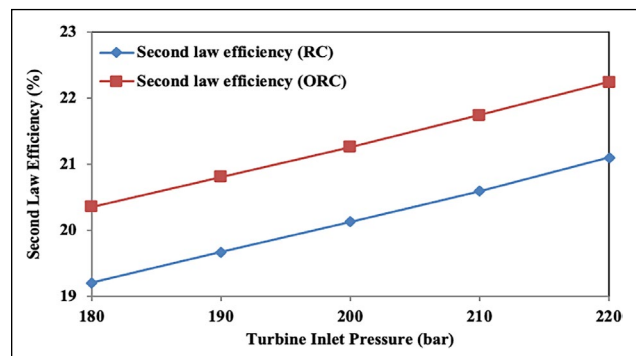


Figure 5. Variations in second law efficiencies with changes in the turbine inlet pressure of the solar tower power plant.

surface temperature of the central receiver. Furthermore, the same increasing trend was noted regarding the first and second law efficiencies of the entire system. The entire cycle efficiency of the second law analysis is also lower than the first law efficiencies as observed for the combined-cycles system. This is due to a major quantity of exergy associated with the thermal energy that has been received being less than its energy content, therefore resulting in lower improvements regarding second law efficiencies for the combined-cycles system for subsequent increases in DNI.

The effect of steam turbine entrance pressure (TIP) on the entire first and then second law efficiencies can be observed in Figures 4 and 5. The computed results indicate that both first and second law efficiencies of the system boosted as TIP increased. The justification for this trend is that an increase in TIP causes an increase in the power outputs in the ORC turbine cycle and in the steam turbine cycle; as a result, the entire first law efficiencies of the model increase. Moreover, the proportion of increment regarding the refrigeration yield of ORC is significantly higher, which ultimately increases the overall power output generated through the steam turbine cycle. However, the behavior of the second law efficiencies increases slightly less when compared with first law efficiencies at the same pressure of the entire system. The primary reason can be stipulated as the exergy related to the heating system being lower than the energy generated through process heat.

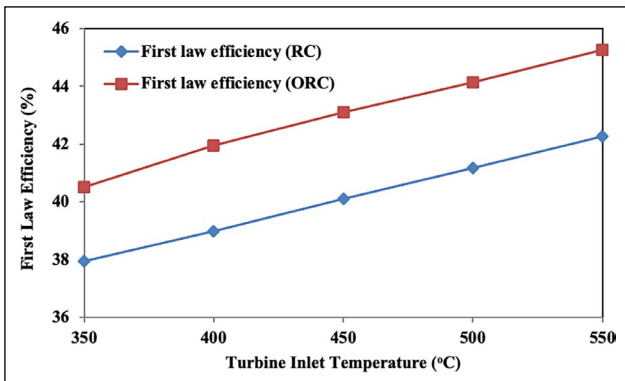


Figure 6. Variations in first law efficiencies with changes in turbine inlet temperature of the solar tower power plant.

RC: Rankine cycle; ORC: Organic Rankine cycle.

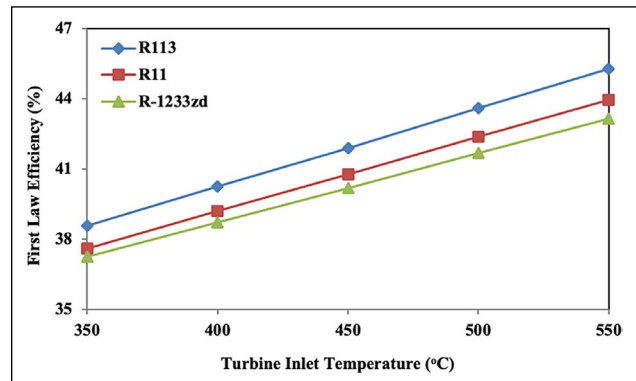


Figure 9. Variations in first law efficiencies for the cycle with changes in turbine inlet temperature at $r_p=25$ bar regarding the different refrigerants for a solar tower power plant.

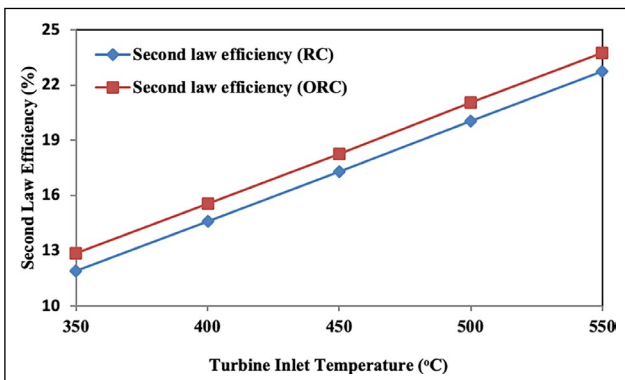


Figure 7. Variations in second law efficiencies with changes in the turbine inlet temperature of the solar tower power plant.

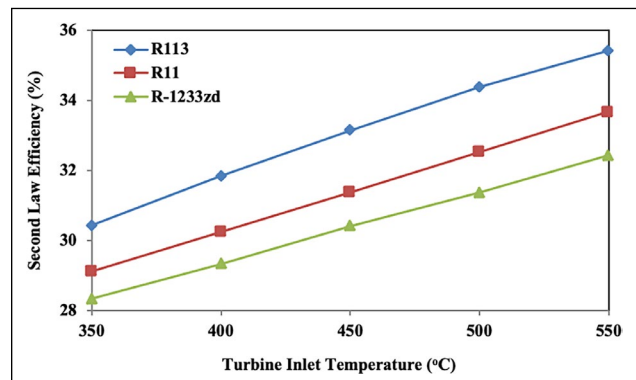


Figure 10. Variations in second law efficiencies of a cycle with changes in turbine inlet temperature at $r_p=25$ bar regarding the different refrigerants of a solar tower power plant.

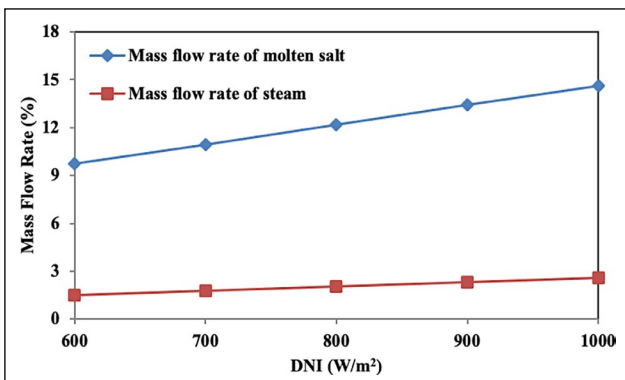


Figure 8. Variations in the mass flow rate of molten salt and steam with changes in DNI for the solar tower power plant.

DNI: Direct normal irradiation.

Figures 6 and 7 display the variations in the first and second law efficiencies of the entire system performance while varying turbine inlet temperature (TIT) for production power. Both first and second law efficiencies of the entire system can be noted to increase appreciably with an increase in TIT of the entire combined-cycles system. This increase was noted as an increase in refrigeration output of ORC and power output from the steam turbine cycle. The findings from the results justify the benefits of integrating ORC with RC, as these show a significant

increment in both first and second law efficiencies of the combined-cycles system, as well as TIT as being an important parameter in the design of a solar-operated organic Rankine cycle system.

The performance regarding the effect from changing the mass flow rate of molten salt and steam generated in the steam generator at different values of DNI is investigated in Figure 8. A model was developed that estimated a rapid gain regarding the mass flow rate of the molten salt, while a simultaneous increase in the mass flow rate of steam was registered when the DNI values increase from 600 W/m² to 1,000 W/m². The reason for the increasing trend of mass flow rate is that increased DNI results in the mass flow rate of molten salt furnishing a high rate of thermal energy to the steam generator. However, the mass flow rate of steam has smaller results compared to the mass flow rate of molten salt in the combined-cycles system.

Figures 9 and 10 display other essential variations detected for the refrigerants R-113, R-11, and R-1233zd in the thermodynamic performance of ORC regarding first and second law efficiencies as TIT increases. As these figures show, the trend is to have higher first and second law efficiencies for all working fluids as TIT increases from 350°C to 550°C. The reason behind this subsequent increase in both first and second law efficiencies is

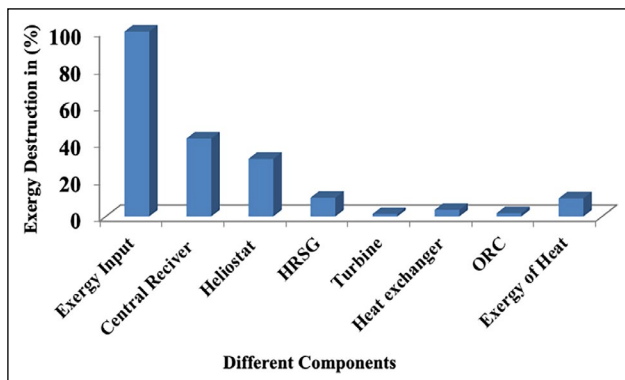


Figure 11. Exergy destruction in each component in the solar tower power plant.

HRSG: Heat recovery steam generator; ORC: Organic Rankine cycle.

primarily due to surplus electric power generation, which is attributed to the bare minimum expansion of the working fluid in the ORC turbine. Conversely, the power produced in the steam turbine is higher than for the above case. Furthermore, a notable increase in the efficiency of R-113 is observed when employed as a heat transfer fluid (refrigerant) in ORC. Concurrently, the fluid appears to possess superior efficiency compared to the R-11 and R-1233zd refrigerants regarding ORC. When comparing the results, R-113 should be noted to have a higher boiling point than both R-11 and R-1233zd, and these results have also been validated by Shah et al. (2020) and Haq (2021).

This section discusses the distribution of exergy destruction for all major components in the system and exergy input to the cycle under consideration (Fig. 11). The central receiver and heliostat have been calculated as having the largest exergy destruction due to the larger temperature differences in the system (42% and 31%, respectively). A substantial quantity of exergy destruction was also noted in the steam generator (around 10%). Among the other components incorporated in the model, an estimated combined exergy destruction of 3% was achieved out of the 100% solar exergy input and has been examined on an individual basis. This exergy destruction analysis provides useful data and also aids designers in generating an order of importance among the components developed for the proposed solar-operated organic Rankine cycle. The results here have also been validated by Ahmad et al. (2022).

6. CONCLUSION

The first and second laws of thermodynamics play a crucial role in analyzing and understanding the performance of power plants and in determining the strategies for limiting losses. Exergy analyses are based on these laws and provide insights into the quality and quantity of energy in a system, thus allowing engineers to identify and minimize losses effectively. The present analysis has established the functional conditions for a

solar-operated steam turbine to recover the waste heat when an organic Rankine cycle (ORC) is integrated at the bottom of a steam Rankine cycle (RC). Keeping the thermodynamics point of view, integrating an RC and an ORC while considering the heat rejected from the steam cycle as waste heat provides much better efficiencies as a result of utilizing the waste heat at the exit for additional power generation. In addition, the current study has introduced a novel concept of uncertainty for obtaining more accurate results with a precision that should remove all human and machine errors. Concluding remarks have been coined from the research as follows:

- A slight gain in first and second law efficiencies was observed after considerably increasing the DNI values under different operating conditions.
- First law efficiencies under the mean operating conditions of DNI occur in the range of 32.31% to 37.99%, and second law efficiencies occur in the range of 24.14% to 25.51% when employing ORC to produce power.
- First law efficiencies are notably increased with increases in turbine inlet pressure, whereas second law efficiencies of a combined-cycles system increase slightly under the same operating conditions.
- First and second law efficiencies are noted to increase slightly as the turbine inlet temperature increases in a combined-cycles system.
- A significant increase in the mass flow rate of molten salt and the mass flow rate of steam was observed as the DNI increased to different values.
- For mean operating conditions, refrigerants used in the ORC cycle show R-113 to rank as the best refrigerant, followed by R-11 in second and R-1233zd in third.
- Of the cycle's 100% exergy input, the greatest exergy destruction was found to be about 42% in the central receiver, 31% in the heliostat, 10% in the steam generator, 3.57% in the heat exchanger, and 1.81% in the ORC.
- Error analysis was applied to remove any uncertainty in the study. The error rate came out to be 3.81%, which is within the desired range.

DATA AVAILABILITY STATEMENT

The published publication includes all graphics and data collected or developed during the study.

CONFLICT OF INTEREST

The author declared no potential conflicts of interest with respect to the research, authorship, and/or publication of this article.

ETHICS

There are no ethical issues with the publication of this manuscript.

FINANCIAL DISCLOSURE

The authors declared that this study has received no financial support.

REFERENCES

- Ahmad, S., Parvez, M., Khan, T. A., Siddiqui, S. A., & Khan, O. (2022). Performance comparison of solar powered cogeneration and trigeneration systems via energy and exergy analyses. *International Journal of Exergy*, 39(4), 395–409. [\[CrossRef\]](#)
- Akram, W., Parvez, M., & Khan, O. (2023). Parametric analysis of solar-assisted trigeneration system based on energy and exergy analyses. *Journal of Thermal Engineering*, 9(3), 764–775. [\[CrossRef\]](#)
- Assad, M., & Rosen, M. (2021). *Design and performance optimization of renewable energy systems* (1st ed.). Academic Press Elsevier. [\[CrossRef\]](#)
- Caraballo, A., Galán-Casado, S., Caballero, A., & Serena, S. (2021). Molten salts for sensible thermal energy storage: a review and an energy performance analysis. *Energies*, 14, Article 1197. [\[CrossRef\]](#)
- Chen, L., Huang, H., Tang, P., Yao, D., Yang, H., & Roohbakhsh, H. (2022). A combined energy system for generating electrical and thermal energies using concentrating solar system, fuel cell and organic Rankine cycle; energy and exergy assessment. *Energy Sources, Part A: Recovery, Utilization, and Environmental Effects*, Article 2043957. [\[CrossRef\]](#)
- Collado, F. J., & Guallar, J. (2019). Quick design of regular heliostat fields for commercial solar tower power plants. *Energy*, 178, 115–125. [\[CrossRef\]](#)
- D'Souza, D., Montes, M. J., Romero, M., & Gonzalez-Aguilar, J. (2023). Energy and exergy analysis of microchannel central solar receivers for pressurised fluids. *Applied Thermal Engineering*, 219, Article 119638. [\[CrossRef\]](#)
- Georges, E., Declaye, S., Dumont, O., Quoilin, S., & Lemort, V. (2013). Design of a small-scale organic Rankine cycle engine used in a solar power plant. *International Journal of Low-Carbon Technologies*, 8(1), i34–i41. [\[CrossRef\]](#)
- Habibi, H., Zoghi, M., Chitsaz, A., Javaherdeh, K., Ayazpour, M., & Bellos, E. (2020). Working fluid selection for regenerative supercritical Brayton cycle combined with bottoming ORC driven by molten salt solar power tower using energy-exergy analysis. *Sustainable Energy Technologies and Assessments*, 39, Article 100699. [\[CrossRef\]](#)
- Haq, M. Z. (2021) Optimization of organic Rankine cycle (ORC) based waste heat recovery (WHR) system using a novel target-temperature-line approach. *Journal of Energy Resources Technology*, 143(9), Article 092101. [\[CrossRef\]](#)
- Holman, J. P. (2012). *Experimental methods for engineers* (8th ed.). Tata McGraw Hill, Series in Mechanical Engineering.
- Hussaini, Z. A., King, P., & Sansom, C. (2020). Numerical simulation and design of multi-tower concentrated solar power fields. *Sustainability*, 12(6), Article 2402. [\[CrossRef\]](#)
- Kerme, E., & Orfi, J. (2015). Exergy-based thermodynamic analysis of solar driven organic Rankine cycle. *Journal of Thermal Engineering*, 1(5), 192–202. [\[CrossRef\]](#)
- Khan, O., Yadav, A. K., Khan, M. E., & Parvez, M. (2021). Characterization of bioethanol obtained from Eichhornia Crassipes plant: Its emission and performance analysis on CI engine. *Energy Sources, Part A: Recovery, Utilization, and Environmental*, 43(14), 1793–1803. [\[CrossRef\]](#)
- Kumar, M. (2020). Social, economic, and environmental impacts of renewable energy resources. *Wind Solar Hybrid Renewable Energy System*. Intech Open. [\[CrossRef\]](#)
- Li, J. (2014). Gradual progress in the organic Rankine cycle and solar thermal power generation. In *Structural optimization and experimental investigation of the organic Rankine cycle for solar thermal power generation*. Springer Theses. [\[CrossRef\]](#)
- Li, Y., Teng, S., & Xi, H. (2023). 3E analyses of a cogeneration system based on compressed air energy storage system, solar collector and organic Rankine cycle. *Case Studies in Thermal Engineering*, 42, Article 102753. [\[CrossRef\]](#)
- Loni, R., Kasaeian, A., Mahian, O., Sahin, A. Z., & Wongwises, S. (2017). Exergy analysis of a solar organic Rankine cycle with square prismatic cavity receiver. *International Journal of Exergy*, 22(2), 103–124. [\[CrossRef\]](#)
- Lourenco, A. B. (2023). Application of the H&S model for the advanced exergy analysis of an organic Rankine cycle. *Revista Ifes Ciência*, 9(1), 1–12. [\[CrossRef\]](#)
- Omar, A., Saghafifar, M., Mohammadi, K., Alashkar, A., & Gadalla, M. (2019). A review of unconventional bottoming cycles for waste heat recovery: Part II – Applications. *Energy Conversion and Management*, 180, 559–583. [\[CrossRef\]](#)
- Parvez, M. (2017). *Steam boiler*. Research Gate.
- Parvez, M., & Khalid, F. (2018). Thermodynamic investigation on sawdust and rice husk biomass integrated gasification for combined power and ejector cooling cycle. *Current Alternative Energy*, 2(1), 19–26. [\[CrossRef\]](#)
- Shah, Z. A., Zheng, Q., Mehdi, G., Malik, A., Ahmad, N., Chanido, M. B., & Waqas, M. (2020). Energy and exergy analysis of regenerative organic Rankine cycle with different organic working fluids. *2020 3rd International Conference on Computing, Mathematics and Engineering Technologies (iCoMET)*. [\[CrossRef\]](#)
- Singh, H., & Mishra, R. S. (2019). Solar thermal collector integrated organic Rankine cycle technology. *Journal of Basic and Applied Engineering Research*, 6(1), 45–48.
- Varis, C., & Ozcira Ozkicil, S. (2023). In a biogas power plant from waste heat power generation system using Organic Rankine Cycle and multi-criteria optimization. *Case Studies in Thermal Engineering*, 44, Article 102729. [\[CrossRef\]](#)

- Vujanović, M., Wang, Q., Mohsen, M., Duić, N., & Yan, J. (2019). Sustainable energy technologies and environmental impacts of energy systems. *Applied Energy*, 256, 113919.
- Yaglı, H., Koç, Y., & Kalay, H. (2021). Optimisation and exergy analysis of an organic Rankine cycle (ORC) used as a bottoming cycle in a cogeneration system producing steam and power. *Sustainable Energy Technologies and Assessments*, 44, Article 100985. [\[CrossRef\]](#)
- Zolfagharnasab, M. H., Aghanajafi, C., Kavian, S., Heydarian, N., & Ahmadi, M. H. (2020) Novel analysis of second law and irreversibility for a solar power plant using heliostat field and molten salt. *Energy Science & Engineering*, 8(11), 4136–4153. [\[CrossRef\]](#)